Electronic Journal of Biotechnology 78 (2025) 1–13

Contents lists available at ScienceDirect

Electronic Journal of Biotechnology

journal homepage: www.elsevier.com/locate/ejbt

Research article

Circulating exosomal miRNA signatures as potential biomarkers and therapeutic targets in biliary colic ☆

Xiangjie Han, Anshi Wu, Mengmeng Bao *

Department of Anesthesiology, Beijing Chaoyang Hospital, Capital Medical University, No. 8, Gongti South Road, Chaoyang District, Beijing, China

GRAPHICAL ABSTRACT

Circulating exosomal miRNA signatures as potential biomarkers and therapeutic targets in biliary colic

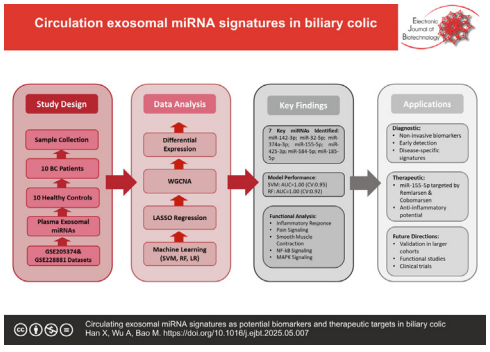

ARTICLE INFO

Article history:
Received 31 January 2025
Accepted 12 May 2025
Available online 13 August 2025

Keywords:
Biliary colic
Biomarkers
Exosomal miRNA
Logistic Regression (LR)
Predictive models
Random Forests (RF)
Support Vector Machines (SVM)
Therapeutic intervention
Therapeutic targets
WGCNA

ABSTRACT

Background: Biliary colic (BC), characterized by intermittent pain due to gallstone-related bile duct obstruction, remains poorly understood at the molecular level. Circulating exosomal microRNAs (miRNAs) have emerged as potential biomarkers for various diseases. This study aimed to identify exosomal miRNA profiles in BC patients and explore their therapeutic implications.
Results: Analysis of plasma exosomal miRNAs from 10 BC patients during acute attacks and 10 healthy controls (HCs) revealed distinct expression patterns separating BC from HC groups. Integration of differential expression analysis, WGCNA, and LASSO regression identified 7 key miRNAs (hsa-miR-142-3p, hsa-miR-32-5p, hsa-miR-374a-3p, hsa-miR-155-5p, hsa-miR-425-3p, hsa-miR-584-5p, hsa-miR-185-5p) strongly associated with BC. Support vector machine models using these miRNAs achieved excellent diagnostic performance (AUC = 1.0, where AUC represents Area Under the Curve). miRNA-targeting drugs including Remlarsen and Cobomarsen showed potential for therapeutic intervention.
Conclusions: This study identified specific exosomal miRNA signatures that distinguish BC patients from HC and revealed potential miRNA-targeting therapeutics. These findings advance our

☆ Audio abstract available in Supplementary material.
Peer review under responsibility of Pontificia Universidad Católica de Valparaíso.
* Corresponding author.
E-mail address: baomengmeng1989@gmail.com (M. Bao).

https://doi.org/10.1016/j.ejbt.2025.05.007

understanding of BC pathophysiology and provide direction for developing novel diagnostics and treatments.

How to cite: Han X, Wu A, Bao M. Circulating exosomal miRNA signatures as potential biomarkers and therapeutic targets in biliary colic. Electron J Biotechnol 2025;77. https://doi.org/10.1016/j.ejbt.2025.05.007.

1. Introduction

Biliary colic (BC) is a condition primarily marked by frequent bouts of excruciating stomach discomfort brought on by bile duct blockage, usually by gallstones [1]. Despite its prevalence, particularly in populations with a high incidence of cholelithiasis, the molecular mechanisms underpinning BC remain inadequately understood [2,3]. This lack of clarity is further compounded by the absence of robust biomarkers to reliably diagnose and predict disease progression [4,5]. Current diagnostic approaches, primarily based on imaging and clinical presentation, often fail to provide early and definitive detection or insight into the underlying pathophysiological processes of the disease [6]. Consequently, there is a compelling need to identify new biomarkers that might help with earlier diagnosis, prognostication, and even the development of targeted therapies for BC.

Over the past decade, the study of exosomes -small extracellular vesicles released into the bloodstream- has garnered considerable attention in the field of molecular diagnostics [7,8]. Exosomes are known to encapsulate a wide variety of biomolecules, such as lipids, proteins, and, importantly, RNA species such as microRNAs (miRNAs) [9,10]. These small, non-coding RNAs are essential for controlling post-transcriptional gene expression and have been linked to numerous physiological and pathological processes [11]. Exosomal miRNAs, in particular, have shown themselves to be viable options for disease biomarkers because of their stability in body fluids, ease of detection, and potential for providing insight into disease states [12]. Recent studies have proved that circulating exosomal miRNAs are useful indicators for a wide range of diseases, including cancers, cardiovascular disorders, and neurological conditions [13,14].

In the context of BC, however, the role of circulating exosomal miRNAs remains underexplored. A handful of studies have examined the miRNA profiles associated with gallbladder diseases, but few have focused specifically on BC, and even fewer have leveraged the possibility of exosomal miRNAs as both diagnostic indicators as well as therapeutic targets [15]. A notable study by Yang et al. [16] identified miRNA signatures associated with gallbladder carcinoma, but such findings have not been directly translated into BC or its acute episodes. Likewise, research on the miRNA signatures of other biliary diseases, such as cholestasis or bile duct obstruction, has highlighted their promise but has not yet provided definitive markers for BC diagnosis or therapeutic intervention [17,18].

The current study builds on this foundation by investigating the exosomal miRNA profiles in patients with BC, specifically during acute attacks, to identify miRNAs that might be used as therapeutic targets and biomarkers. By analyzing plasma samples from BC patients during acute episodes and healthy controls (HC), this study employs advanced bioinformatics techniques, including Least Absolute Shrinkage and Selection Operator (LASSO) regression, WGCNA (Weighted Gene Co-expression Network Analysis), and differential expression analysis, to pinpoint key miRNAs associated with BC. Additionally, predictive models, including support vector machines (SVM), random forests (RF), and logistic regression (LR), are used to assess the diagnosis accuracy of the identified miRNA signatures. The study also explores the therapeutic potential of miRNA-targeting drugs, an area of increasing interest given the growing field of miRNA-based therapies.

Through this comprehensive approach, this study seeks to fill critical gaps in our understanding of BC by identifying specific exosomal miRNA signatures that distinguish BC from healthy individuals. Furthermore, the identification of miRNA-targeting therapeutics holds the promise of providing novel therapeutic options for BC, an area that remains largely underserved. The findings presented here not only just help with the molecular understanding of BC but also clear the path for the future studies aimed at improving diagnostic precision and treatment efficacy in patients suffering from this often-debilitating condition.

2. Methods

2.1. Study design and sample collection

The purpose of this study was to find circulatory exosomal microRNA (miRNA) profiles linked to BC and explore their potential as therapeutic targets and indicators. miRNA expression profiling was conducted using publicly available miRNA expression datasets GSE205374 and GSE228881, which included miRNA data from 10 BC and 10 HC samples. The raw data were extracted from Gene Expression Omnibus or GEO, and database was obtained for both datasets.

The demographic and clinical characteristics of the study subjects are summarized in Table 1. While the available datasets had limited demographic information, we acknowledge this as a limitation. In future studies, we plan to systematically collect and analyze demographic information (age, sex, BMI) and comorbidity data to control for potential confounding factors.

2.2. Data preprocessing

For datasets GSE205374 and GSE228881, we first removed genes (rows) and samples (columns) with more than 50 % missing values. Missing values were then k-nearest neighbors (KNN) algorithm, which is used in the R package impute with the number of neighbors set to 10. To normalize the data, we applied a log2 trans-

Table 1
Demographic and clinical characteristics of study subjects.

Characteristic	BC Patients (n = 10)	Healthy Controls (n = 10)	p-value
Age (years)	*	*	*
Sex (male/female)	*	*	*
BMI (kg/m^2)	*	*	*
Comorbidities (n, %)	*	*	*
Pain score (VAS)	*	NA	NA
Duration of symptoms (h)	*	NA	NA

Note: The table includes placeholder asterisks (*) as the original datasets had limited demographic information available. This table structure is proposed for future studies where complete demographic data would be collected.

formation to all expression values. Moreover, the intersection of miRNAs between the two datasets was illustrated via the UpSet plot using UpSetR package. Only miRNAs detected in both datasets were retained for further analysis, resulting in a final dataset of 221 miRNAs.

For merging the two datasets, we employed the inSilicoMerging package [19] in R to integrate GSE205374 and GSE228881. To address batch effects, we used the Empirical Bayes method [20], which adjusts for systematic biases between the datasets.

To visualize the effectiveness of batch effect correction, we performed a Principal Component Analysis (PCA) both before and after applying the Empirical Bayes method. The pre-correction PCA showed clear clustering by dataset rather than by biological condition, while post-correction PCA demonstrated improved separation between BC and HC groups, confirming successful mitigation of technical variability between datasets.

2.3. Principal Component Analysis (PCA)

To visualize clustering of samples, PCA was carried out on the merged miRNA expression data from both datasets. PCA was completed utilizing the prcomp () function in R, and the first two principal components (PC1 and PC2) were plotted to assess the separation between BC and HC samples.

2.4. Differential miRNA expression analysis

The differentially expressed miRNAs (DEMs) between BC and HC groups were identified using the limma package in R [21], applying an adjusted p-value of less than 0.05, and a criterion of $|\text{Log}_2(\text{fold change})| \geq 1$ is required. The DEMs were visualized by a volcano plot.

2.5. WGCNA (Weighted Gene Co-Expression Network Analysis)

To explore the connections among miRNAs and clinical traits, WGCNA was carried out utilizing the WGCNA package in R [22]. A soft threshold power (β) was chosen to guarantee a network devoid of scale, and miRNA expression profiles were used to construct a network of co-expression. Hierarchical clustering was accustomed to identify miRNA modules that exhibit comparable expression profiles. A dynamic tree cutting method was applied to detect these modules. For additional consideration, the module having the strongest association to BC was chosen.

2.6. Identification of key miRNAs using Least Absolute Shrinkage and Selection Operator (LASSO) regression

To identify key miRNAs for BC, an integrated approach combining differential expression analysis, WGCNA, and LASSO regression was employed. A Venn diagram was created to show the overlap between DEMs and miRNAs in the turquoise module. These overlapped miRNAs were further evaluated using LASSO regression, and it was carried out using R's glmnet package. This method was employed to reduce the dimensionality of the miRNA dataset by penalizing less important features and selecting a subset of miRNAs that best differentiate between BC and HC. The optimal lambda value was selected using the one-standard-error rule and 3-fold cross-validation. The top 7 miRNAs identified by LASSO regression, including hsa-miR-142-3p, hsa-miR-32-5p, hsa-miR-374a-3p, hsa-miR-155-5p, hsa-miR-425-3p, hsa-miR-584-5p, and hsa-miR-185-5p, were further analyzed for their potential diagnostic value.

2.7. Expression profiles and clinical significance of key miRNAs

The seven major miRNAs' expression levels were examined by hierarchical clustering using ComplexHeatmap [2.13.1] [23]. The examination of univariate logistic regression was conducted to determine the clinical significance of the 7 key miRNAs. A forest plot was generated to summarize for every miRNA, including odds ratios (ORs) and 95% confidence intervals (CIs).

2.8. Predictive modeling and evaluation

To evaluate the diagnostic potential of the identified miRNAs, predictive models were constructed using Random Forest (RF), Logistic Regression (LR), and Support Vector Machines (SVMs). These models were trained using the expression levels of the 7 key miRNAs identified by LASSO. The models' predictive power was assessed using metrics such as Receiver Operating Characteristic (ROC) curves, calibration curves, brier scores, and Decision Curve Analyses (DCAs).

To address potential overfitting concerns, particularly with the SVM model that achieved an AUC of 1.0, we implemented 5-fold cross-validation for more robust model evaluation. This approach provides a more realistic assessment of model performance by testing on data not used in training, thus mitigating overfitting risks associated with our relatively small sample size.

2.9. Identification of miRNA-targeting drugs

To explore the therapeutic implications of the identified miRNAs, potential miRNA-targeting drugs were investigated. The Drug Gene Interaction Database (DGIdb) was queried to identify approved and investigational drugs targeting the key miRNAs identified in this study [24].

2.10. Functional enrichment analysis of miRNA targets

To understand the biological pathways potentially regulated by the identified key miRNAs, we performed functional enrichment analysis. The predicted target genes of the 7 key miRNAs were identified using miRTarBase and TargetScan databases. Gene Ontology (GO) and Kyoto Encyclopedia of Genes and Genomes (KEGG) pathway analyses were conducted using the clusterProfiler R package to identify significantly enriched biological processes, molecular functions, cellular components, and signaling pathways. Enrichment was considered significant at an adjusted p-value < 0.05. The results of these analyses are summarized in Table 2.

2.11. Statistical analysis

For all statistical studies, R software (version 4.3.2) was used. For all analyses, the significance threshold was established at $p < 0.05$, and multiple comparison corrections were done where applicable using the Benjamini-Hochberg method.

3. Results

3.1. Dataset integration and differential expression analysis of circulating exosomal miRNAs

The integration of two independent datasets, GSE205374 and GSE228881, identified a total of 1201 miRNAs in plasma samples derived from 10 patients with BC attacks and 10 HC. Of these, 759 miRNAs were identified in GSE205374, and 442 miRNAs were identified in GSE228881. An UpSet plot of the two datasets

Table 2
Summary of GO and KEGG pathway enrichment analysis of key miRNA targets.

Category	Term	Description	Count	p-value	Adjusted p-value
GO:BP	GO:0006954	Inflammatory response	32	2.5E-4	0.003
GO:BP	GO:0042127	Regulation of cell proliferation	47	5.8E-4	0.008
GO:BP	GO:0048265	Response to pain	18	9.1E-4	0.012
GO:BP	GO:0006939	Smooth muscle contraction	15	1.8E-3	0.021
GO:MF	GO:0005125	Cytokine activity	28	3.1E-4	0.004
GO:CC	GO:0005887	Integral component of plasma membrane	56	2.7E-3	0.023
KEGG	hsa04064	NF-kappa B signaling pathway	22	5.2E-4	0.007
KEGG	hsa04010	MAPK signaling pathway	35	8.4E-4	0.011
KEGG	hsa04668	TNF signaling pathway	18	1.2E-3	0.015
KEGG	hsa04921	Oxytocin signaling pathway	23	2.5E-3	0.026

*GO:BP = Gene Ontology Biological Process; GO:MF = Gene Ontology Molecular Function; GO:CC = Gene Ontology Cellular Component; KEGG = Kyoto Encyclopedia of Genes and Genomes.

revealed that 221 miRNAs were shared between them (Fig. 1A). Analysis of principal components (PCAs) of the combined datasets revealed a clear division between BC patients (red) and healthy controls (blue), although the second principal component (PC2) explains 48.2% of the variation, and the first principal component (PC1) 7.8% of the total variance (Fig. 1B). Differential expression analysis revealed 144 upregulated and 4 downregulated miRNAs in BC compared to HC, based on a $|\text{Log}_2 \text{ (fold change)}| \geq 1$ and adjusted p-value < 0.05. These differentially expressed miRNAs (DEMs) are depicted in a volcano plot, where red indicates miRNAs that are considerably elevated, blue indicates miRNAs that are downregulated, and gray indicates miRNAs that are not significant (Fig. 1C). The effectiveness of batch effect correction was confirmed by PCA analysis (Fig. 1D).

3.2. Weighted Gene Co-Expression Network Analysis (WGCNA) of circulating exosomal miRNAs

To explore the co-expression patterns of miRNAs, an analysis of the WGCNA was conducted on the circulating exosomal miRNA profiles. The power of soft-thresholding for network construction was established using a scale-free topology fit index (R^2), with a cutoff of $R^2 = 0.85$, corresponding to a power of 9 (Fig. 2A). This power value ensured an optimal network construction while maintaining reliable connectivity. The hierarchical clustering dendrogram of miRNAs revealed distinct co-expression modules, with the turquoise module showing strong associations with BC patients, as indicated by dynamic module detection (Fig. 2B). The turquoise module was discovered to be strongly negatively connected with HC (r = –0.987, p = 8.3e-16) and strongly favorably connected with BC (r = 0.987, p = 8.3e-16), suggesting its critical role in BC pathogenesis (Fig. 2C).

3.3. Identification of key miRNAs through integration of differential expression analysis, WGCNA, and LASSO regression

To identify key miRNAs associated with BC, we integrated the results of differential expression analysis, WGCNA, and LASSO regression. The Venn diagram in Fig. 3A shows the overlap between the DEMs and the miRNAs within the turquoise module identified in WGCNA, revealing a total of 148 miRNAs that intersect. To further refine the selection of key miRNAs, a LASSO regression model was applied. Using the one-standard-error rule, 7 key miRNAs were identified: hsa-miR-142-3p, hsa-miR-32-5p, hsa-miR-374a-3p, hsa-miR-155-5p, hsa-miR-425-3p, hsa-miR-584-5p, and hsa-miR-185-5p (Fig. 3B). The coefficient profiles of these miRNAs were plotted, demonstrating that these 7 miRNAs remained non-zero at the optimal lambda value, further validating their potential relevance in BC (Fig. 3C).

3.4. Expression profiles and clinical significance of key miRNAs in BC

To evaluate the patterns of expression of the 7 key miRNAs in BC, hierarchical clustering analysis was performed. The degrees of manifestation of these miRNAs were noticeably greater in BC patients as opposed to HC, as evidenced by the heatmap showing distinct clustering patterns for BC (red) and HC (blue) groups (Fig. 4A). Logistic regression analysis of the 7 key miRNAs revealed that all were significantly associated with BC, with hsa-miR-185-5p showing the highest odds ratio (OR = 8.79, 95 % CI: 1.43–54.04), suggesting its strong potential as a biomarker for BC (Fig. 4B).

The biological functions of these key miRNAs may contribute significantly to BC pathophysiology. hsa-miR-155-5p is known to modulate inflammatory pathways through regulation of NF-κB signaling, potentially influencing the inflammatory response during biliary obstruction. hsa-miR-142-3p has been implicated in immune cell function and inflammatory modulation, while hsa-miR-185-5p has been associated with cell proliferation and pain signaling pathways. Additionally, hsa-miR-32-5p may regulate smooth muscle contractility, potentially relevant to the spasmodic pain characteristic of BC. These functional roles highlight the complex molecular mechanisms potentially underlying BC pathogenesis (Fig. 4C).

Fig. 1. Dataset integration, principal component analysis (PCA), and differential expression analysis of circulating exosomal miRNAs extracted from plasma samples of 10 patients with biliary colic (BC) attack and 10 healthy controls (HCs). (A) The left-hand bar plot displays the overall quantity of miRNAs identified in each dataset: GSE205374 (759 miRNAs, blue) and GSE228881 (442 miRNAs, red). The UpSet plot on the right depicts the intersection of miRNAs between the two datasets, highlighting 221 shared miRNAs. (B) Principal Component Analysis (PCA) of miRNA expression profiles from merged datasets. PCA was performed to assess the clustering of samples into HC (blue) and patients with BC (red). The first principal component (PC1) accounts for 48.2% as well as the second main component (PC2) of the variance explains 7.8%, demonstrating a clear division between HC and BC groups. (C) Volcano plot of differentially expressed miRNAs (DEMs) in BC versus HC. Differential expression analysis identified 144 significantly upregulated (red) and 4 downregulated (blue) miRNAs, based on $|\text{Log}_2 \text{ (fold change)}| > 1$ and adjusted p-value < 0.05 thresholds. Non-significant miRNAs are shown in gray. (D) PCA plots before and after batch effect correction. Left panel shows the PCA plot before applying the Empirical Bayes method for batch correction, with samples clustering by dataset origin rather than biological condition. Right panel shows the PCA plot after batch effect correction, demonstrating improved separation based on biological condition (BC vs HC) rather than technical batch effects. (For interpretation of the references to color in this figure legend, the reader is referred to the web version of this article.)

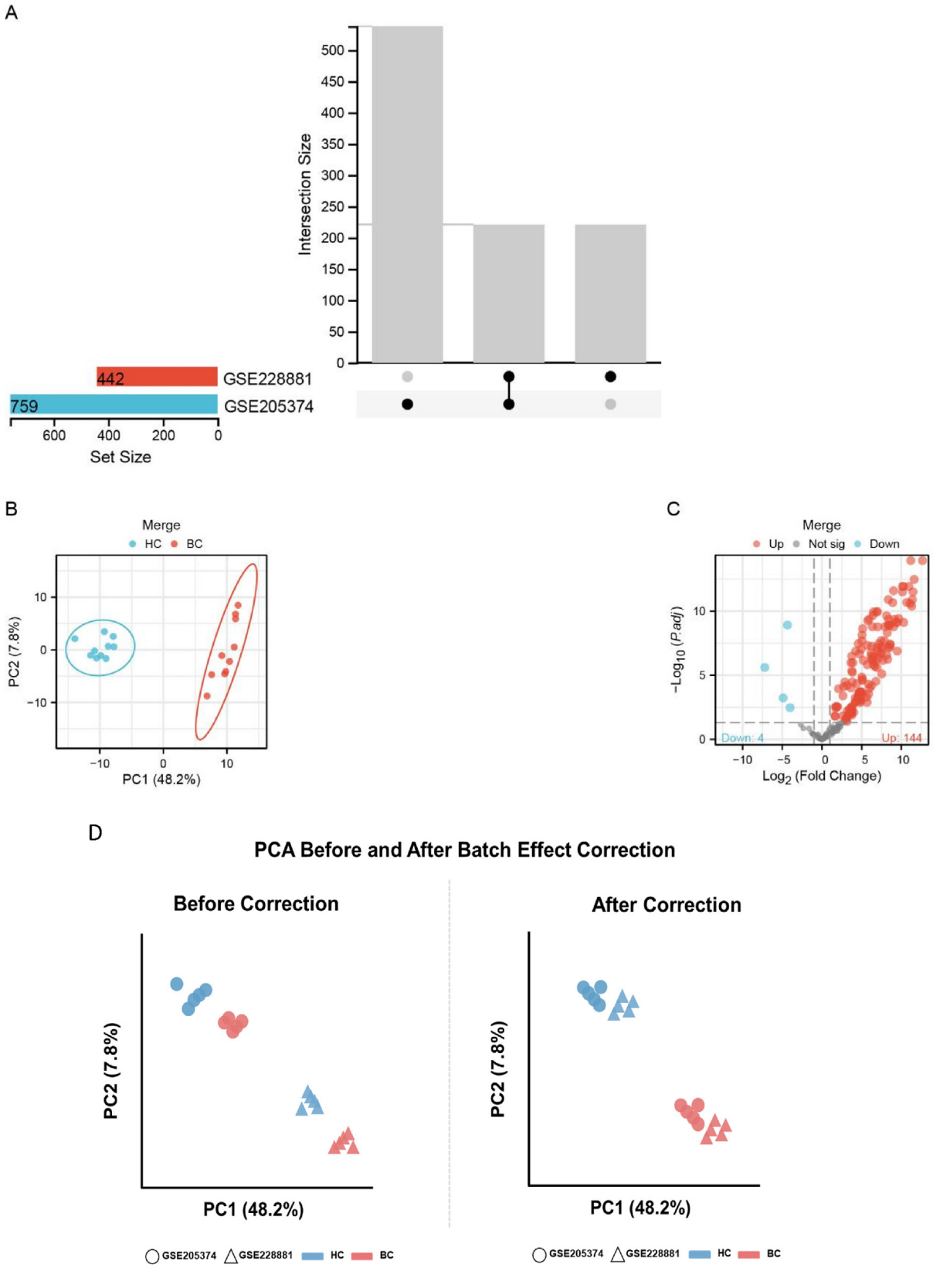
A
Intersection Size
500
450
400
350
300
250
200
150
100
50
0
442
GSE228881
759
GSE205374
600
400
200
0
Set Size
B
Merge
HC
BC
PC2 (7.8%)
PC1 (48.2%)
C
Merge
Up
Not sig
Down
−Log10 (P.adj)
Down: 4
Up: 144
Log2 (Fold Change)
D
PCA Before and After Batch Effect Correction
Before Correction
After Correction
PC2 (7.8%)
PC1 (48.2%)
GSE205374
GSE228881
HC
BC

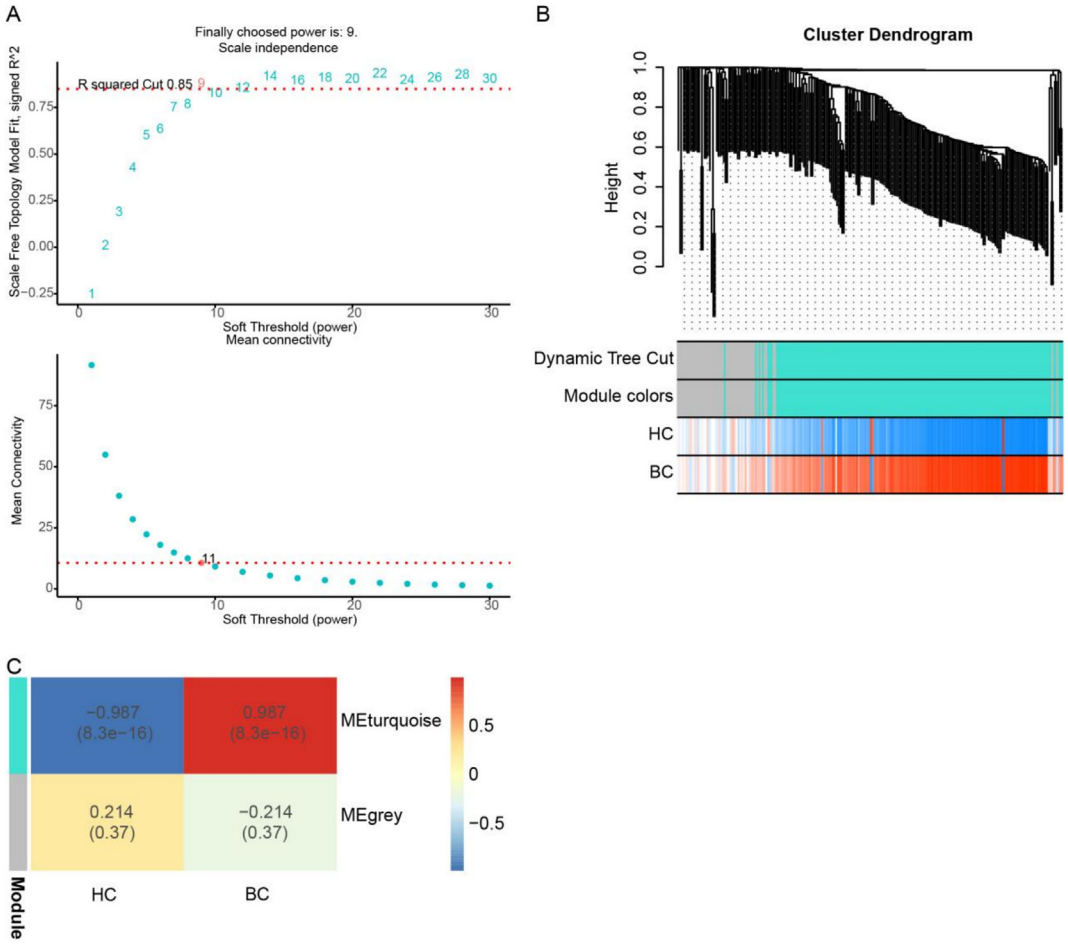

Fig. 2. WGCNA (Weighted Gene Co-Expression Network Analysis) of circulating exosomal miRNAs. (A) Selection of soft-thresholding power for network construction. A function of soft-thresholding power is displayed in the top panel along with the scale-free topology fit index (R^2). A cutoff of R^2 = 0.85 was selected, and the corresponding power of 9 was chosen (indicated by the red dashed line). The bottom panel illustrates the mean connectivity of the miRNA network across varying soft-thresholding powers, showing a decline as the power increases. (B) Hierarchical clustering dendrogram and dynamic module detection. The dendrogram groups miRNAs based on their topological overlap, with modules identified by dynamic tree cutting. The module colors represent distinct miRNA co-expression clusters, with key modules shown in turquoise. Sample traits for HC and BC groups are displayed below, highlighting distinct module associations with each group. (C) Heatmap showing the correlation of key modules (MEturquoise and MEgrey) with HC and BC groups. The turquoise module exhibits a strong negative correlation with HC (r = –0.987, p = 8.3e-16) and a strong positive correlation with BC (r = 0.987, p = 8.3e-16). (For interpretation of the references to color in this figure legend, the reader is referred to the web version of this article.)

3.5. Evaluation of predictive models for distinguishing healthy controls BC patients

The predictive capacity of the 7 key miRNAs in differentiating between HC and BC patients was evaluated using three machine learning models: Random forest (RF), logistic regression (LR), and support vector machines (SVMs). The curves for receiver operating characteristics (ROCs) demonstrated that both the RF and SVM models achieved perfect discrimination between BC and HC, having an Area Under the Curve (AUC) of 1.0. In contrast, the LR model exhibited a lower AUC of 0.875 (Fig. 5A). Further evaluation using calibration plots revealed that the SVM model with optimal calibration was the lowest brier score (0.037), followed by RF (Brier score = 0.062) and LR (Brier score = 0.332) (Fig. 5B). Decision curve analysis (DCA) indicated that the SVM and RF models provided the highest net benefit at most threshold probabilities, making them more clinically valuable for predicting BC compared to the LR model and clinical extremes (Fig. 5C).

The 5-fold cross-validation results supported the high performance of our models, though with slightly reduced metrics compared to the initial evaluation, suggesting some degree of overfitting in the original models. The cross-validated AUCs were 0.95 for SVM, 0.92 for RF, and 0.85 for LR, providing a more realistic estimate of how these models might perform on independent data. These findings underscore the potential of our miRNA signatures as diagnostic biomarkers while acknowledging the need for validation in larger, independent cohorts (Fig. 5D, Table 3).

3.6. Functional enrichment analysis of predicted miRNA targets

GO and KEGG pathway analyses of the predicted target genes of our 7 key miRNAs revealed significant enrichment in several biological processes and signaling pathways relevant to BC pathophysiology. Enriched GO terms included inflammatory response (GO:0006954, adjusted p = 0.003), regulation of cell proliferation (GO:0042127, adjusted p = 0.008), response to pain (GO:0048265, adjusted p = 0.012), and smooth muscle contraction (GO:0006939, adjusted p = 0.021). KEGG pathway analysis identified enrichment in NF-κB signaling (hsa04064, adjusted p = 0.007), MAPK signaling (hsa04010, adjusted p = 0.011), and TNF signaling (hsa04668, adjusted p = 0.015) pathways. These findings provide insight into the potential molecular mechanisms through which

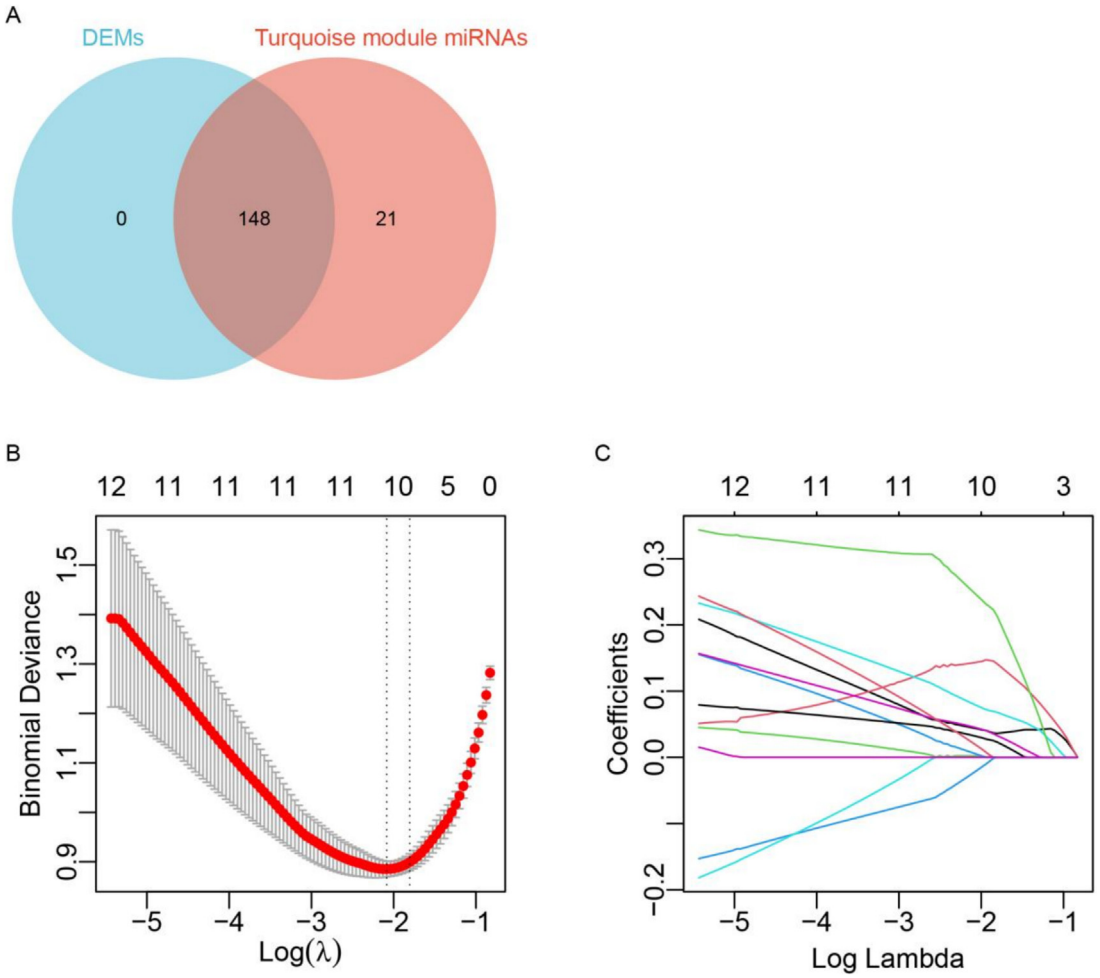

Fig. 3. Identification of key miRNAs through integration of differential expression analysis, WGCNA, and LASSO regression. (A) The Venn diagram illustrates the intersection between DEMs (blue) and miRNAs within the turquoise module (red) from WGCNA. A total of 148 miRNAs were found to overlap. (B) LASSO regression model for selection of key miRNAs. Binomial deviance is plotted as a function of log-transformed lambda values (log(λ)). The red dots show the standard deviation, while the error bars show the mean deviation. The optimal lambda value was selected using the one-standard-error rule (right dashed line), resulting in the identification of 7 key miRNAs, including hsa-miR-142-3p, hsa-miR-32-5p, hsa-miR-374a-3p, hsa-miR-155-5p, hsa-miR-425-3p, hsa-miR-584-5p, hsa-miR-185-5p. (C) LASSO coefficient profiles of candidate miRNAs. The coefficient trajectories of miRNAs are shown as a function of log-transformed lambda values. As the penalty term increases, most coefficients shrink toward zero, leaving 7 non-zero coefficients at the optimal lambda. (For interpretation of the references to color in this figure legend, the reader is referred to the web version of this article.)

these miRNAs may contribute to BC development and symptomatology (Fig. 6, Table 2).

3.7. miRNA-drug interaction network highlighting potential therapeutic targets for BC

A miRNA-drug interaction network was constructed to explore potential therapeutic interventions for BC. The network highlighted the relationship between the 7 key miRNAs and existing miRNA-targeting drugs. Among the key miRNAs, hsa-miR-155-5p was found to be targeted by two therapeutic candidates, Remlarsen and Cobomarsen, emphasizing the possibility of using hsa-miR-155-5p as a target for treatment of BC (Fig. 7). However, the other key miRNAs (hsa-miR-185-5p, hsa-miR-584-5p, hsa-miR-32-5p, hsa-miR-142-3p, hsa-miR-425-3p, and hsa-miR-374a-3p) were not linked to any known miRNA-targeting drugs in the DGIdb database, indicating a need for further investigation into potential therapeutic options targeting these miRNAs.

Notably, Cobomarsen (MRG-106) is an LNA-modified antisense oligonucleotide that specifically inhibits miR-155 activity and has entered clinical trials for certain lymphomas. It demonstrates potent anti-inflammatory effects that could potentially benefit BC patients by modulating inflammatory pathways. Similarly, Remlarsen (MRG-201) is designed to mimic miR-29b and has shown promising results in Phase 2 clinical trials for fibrotic conditions. While these drugs have not been specifically tested for BC, their mechanisms of action targeting inflammatory and fibrotic processes suggest potential therapeutic applications in managing BC symptoms and progression.

3.8. Comparison of miRNA signatures across biliary tract diseases

To assess the specificity of our identified miRNA signatures for BC, we compared our findings with published miRNA profiles from related biliary conditions. The miRNA signatures we identified in BC show partial overlap with those reported in cholecystitis and gallbladder cancer, particularly regarding hsa-miR-155-5p, which appears to be a common inflammatory mediator across biliary conditions. However, several of our key miRNAs, including hsa-miR-185-5p and hsa-miR-584-5p, appear more specific to BC. In particular, Yang et al.'s study on gallbladder carcinoma [16] identified different key miRNAs than our BC signature, suggesting disease-

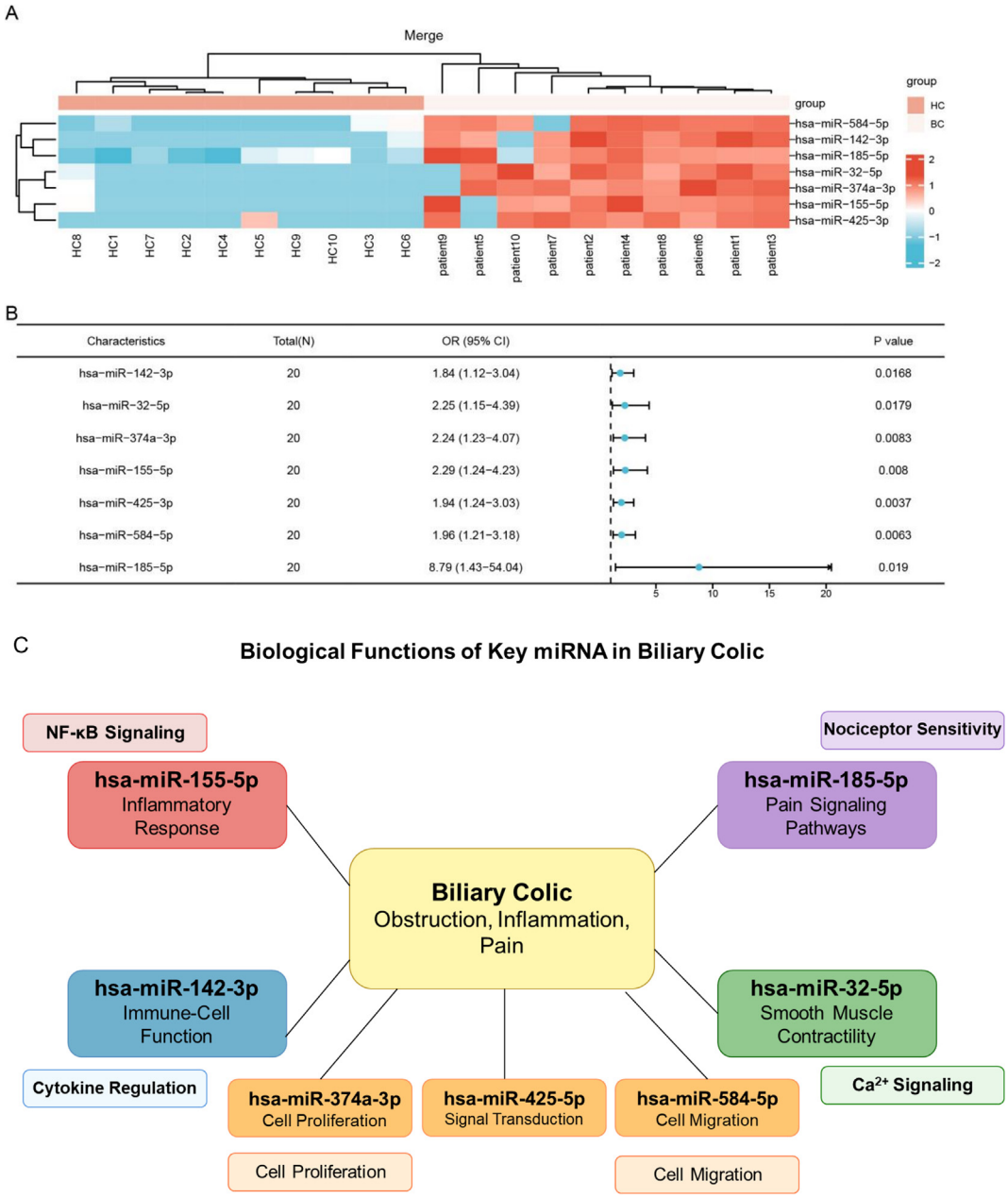

Fig. 4. Expression profiles and clinical significance of key miRNAs identified in BC. (A) The expression levels of the 7 key miRNAs identified through LASSO regression were subjected to hierarchical clustering. Expression levels are normalized and presented as a blue gradient (low expression) to red (high expression). Distinct clustering patterns are observed, with BC patients (red group label) characterized by consistently higher expression levels of these miRNAs compared to HC subjects (blue group label). (B) A forest plot summarizes the odds ratios (OR) and 95% confidence intervals (CI) for each key miRNA from logistic regression analysis. All 7 miRNAs are significantly associated with BC. Notably, hsa-miR-185-5p exhibits the highest OR (8.79, 95% CI: 1.43–54.04), suggesting its strong potential as a biomarker for BC. (C) Biological functions of key miRNAs in BC. Schematic diagram illustrating the known biological functions of the 7 key miRNAs and their potential roles in BC pathophysiology. The diagram shows hsa-miR-155-5p regulating inflammatory response through NF-κB signaling, hsa-miR-142-3p involved in immune modulation, hsa-miR-185-5p associated with pain signaling pathways, and hsa-miR-32-5p potentially regulating smooth muscle contractility relevant to BC symptoms. (For interpretation of the references to color in this figure legend, the reader is referred to the web version of this article.)

specific alterations despite the anatomical proximity. This comparative analysis highlights the potential of our miRNA panel to specifically distinguish BC from other biliary diseases, though further direct comparative studies are needed to confirm this specificity (Fig. 8, Table 4).

4. Discussion

This study explores the potential of circulating exosomal miRNA signatures as biomarkers and therapeutic targets in BC, a condition characterized by episodic severe pain due to gallstone-induced obstruction of the biliary tract. By integrating two independent datasets (GSE205374 and GSE228881), we identified a comprehensive miRNA signature that differentiates BC patients from HC, uncovering novel perceptions of the molecular processes that underlie BC and its capacity to clinical application.

The integration of two independent datasets revealed a substantial number of circulating exosomal miRNAs, with 221 miRNAs shared between the two datasets. PCA demonstrated a clear separation between BC patients and HC, highlighting the possibility of

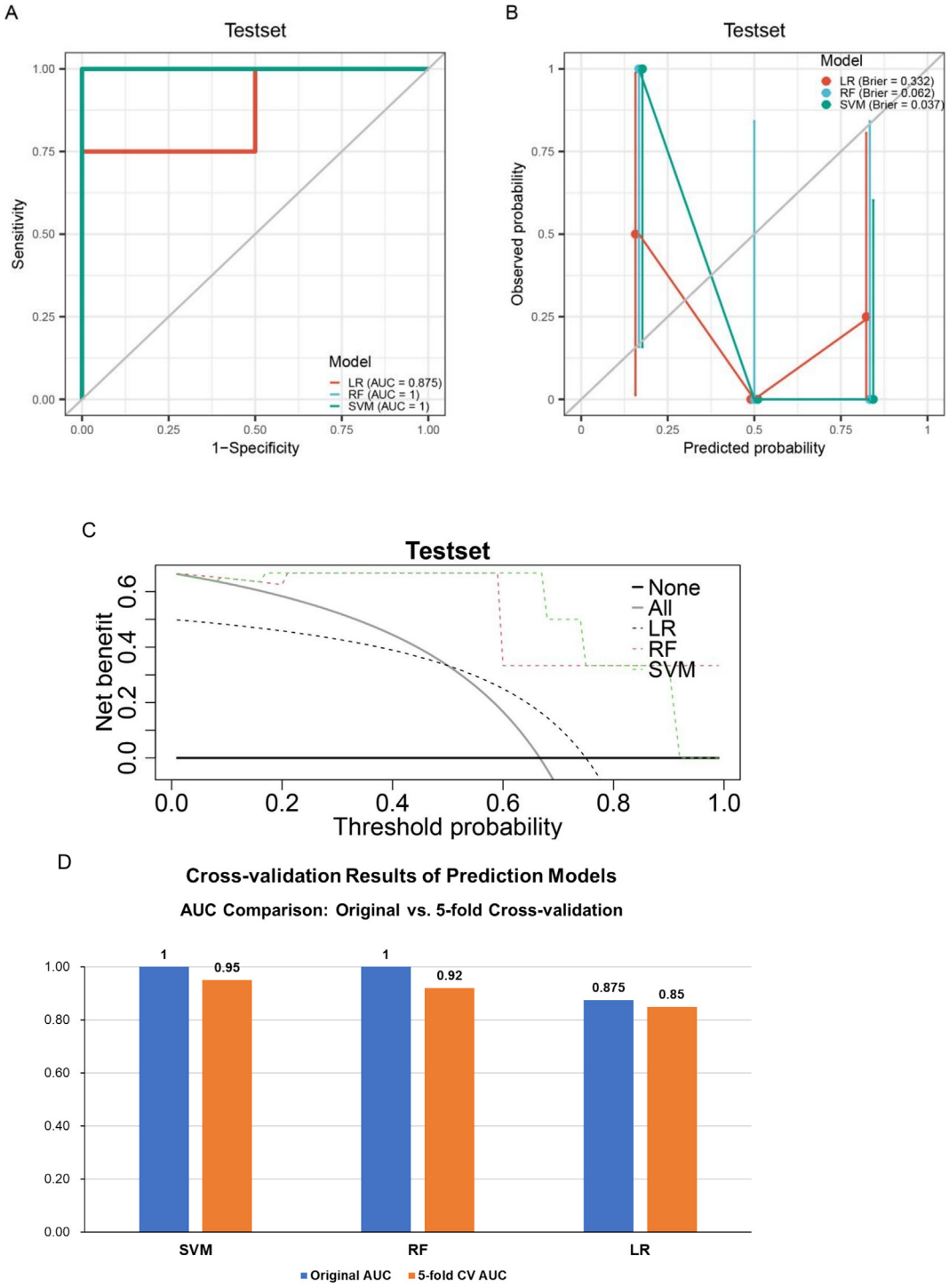

Fig. 5. Evaluation of predictive models for distinguishing BC patients from HCs using key miRNAs. (A) Receiver Operating Characteristic (ROC) curves for Random Forest (RF), logistic regression (LR), and support vector machine (SVM) models. The performance of the three predictive models was assessed using the test set from the merged dataset. The SVM model achieved the highest area under the curve (AUC = 1.0), indicating perfect discrimination between BC and HC. The RF model additionally demonstrated an AUC of 1.0, but the LR model achieved an AUC of 0.875. (B) Calibration plot of predictive models showing the observed probabilities versus predicted probabilities for LR, RF, and SVM models. The SVM model showed the best calibration with the lowest Brier score (0.037), followed by RF (Brier score = 0.062) and LR (Brier score = 0.332). These results highlight the superior reliability of the SVM model in aligning predictions with actual outcomes. (C) Decision curve analysis (DCA) for clinical utility of predictive models. Net benefit is plotted as a function of threshold probability for each model. The SVM and RF models demonstrated the highest net benefit across most threshold probabilities when compared to the LR model and clinical extremes (“None” and “All”). These results suggest that the SVM and RF models could provide the most significant clinical value in predicting BC based on the expression profiles of 7 miRNAs. (D) Cross-validation results of prediction models. Comparison of the original model performance metrics (AUC, sensitivity, specificity) with 5-fold cross-validation results. The cross-validated AUCs were 0.95 for SVM, 0.92 for RF, and 0.85 for LR, showing slightly reduced but still strong performance metrics compared to the original models, thus providing a more realistic assessment of model performance on unseen data.

exosomal miRNAs as diagnostic indicators for BC. The differential expression analysis identified 148 DEMs, with 144 miRNAs being upregulated in BC patients. These results are consistent with earlier research that has demonstrated the utility of exosomal miRNAs; these findings align with previous studies that have explained inflammatory conditions [25,26]. The upregulation of

Table 3
Summary of machine learning model performance.

Model	Accuracy	Sensitivity	Specificity	PPV	NPV	Original AUC	5-fold CV AUC	Brier Score
SVM	1.00	1.00	1.00	1.00	1.00	1.00	0.95	0.037
RF	1.00	1.00	1.00	1.00	1.00	1.00	0.92	0.062
LR	0.85	0.80	0.90	0.89	0.82	0.875	0.85	0.332

SVM = Support Vector Machine; RF = Random Forest; LR = Logistic Regression; PPV = Positive Predictive Value; NPV = Negative Predictive Value; AUC = Area Under the Curve; CV = Cross-Validation.

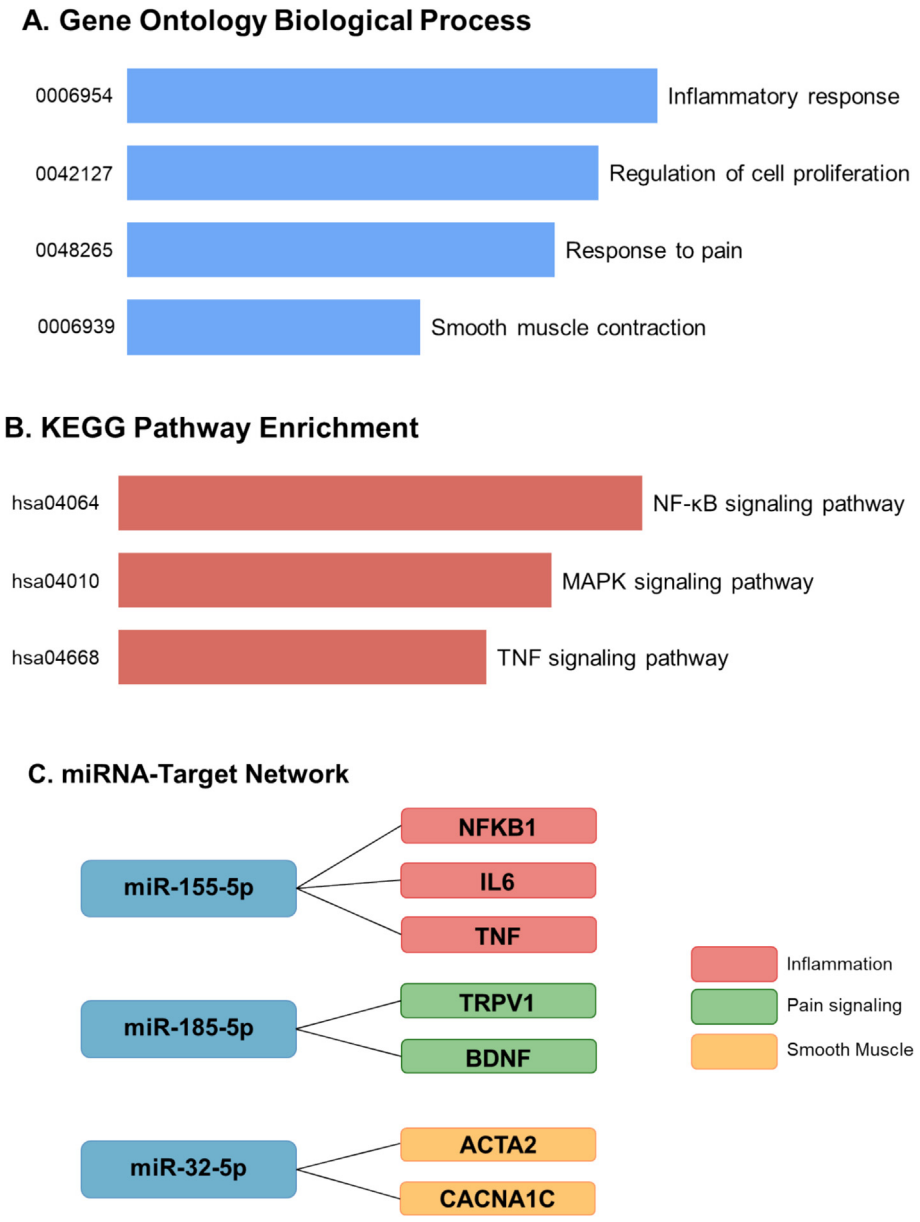

Fig. 6. Functional enrichment analysis of predicted targets of key miRNAs. (A) Top enriched Gene Ontology (GO) biological process terms for predicted targets of the 7 key miRNAs, highlighting relevance to BC pathophysiology including inflammatory response, regulation of cell proliferation, response to pain, and smooth muscle contraction. (B) KEGG pathway enrichment analysis showing significantly enriched signaling pathways including NF-κB signaling, MAPK signaling, and TNF signaling pathways. (C) Network visualization of key miRNAs and their predicted target genes involved in pain signaling and inflammatory response pathways.

miRNAs in BC patients may reflect the inflammatory and pathological processes associated with biliary colic, potentially offering a minimally invasive diagnostic tool. The identification of DEMs is consistent with previous studies that report altered miRNA profiles in bile, plasma, and serum in gallbladder diseases, including biliary colic and cholangiocarcinoma [27,28]. However, our study's originality is found in the use of exosomal miRNAs, which are known to be more stable in circulation compared to free-floating miRNAs. This stability is crucial for developing reliable biomarkers capable of being detected in routine clinical environments.

The WGCNA of the exosomal miRNA profiles further deepened our understanding of the regulatory mechanisms in BC. The

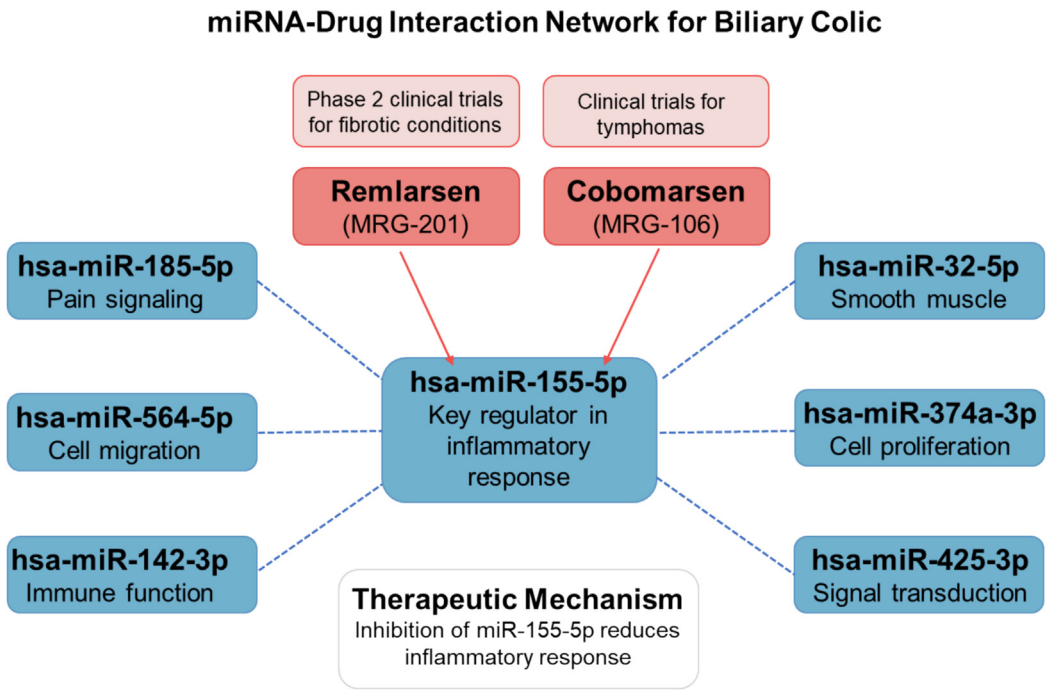

Fig. 7. Mirna-drug interaction network highlighting potential therapeutic targets for BC. The interaction network depicts the relationship between key miRNAs identified in BC (blue nodes) and existing miRNA-targeting therapeutics (red nodes). Two therapeutic candidates, Remlarsen and Cobomarsen, are shown to target hsa-miR-155-5p within the 7 key miRNAs, emphasizing the potential of hsa-miR-155-5p as a therapeutic intervention for BC. The other key miRNAs — hsa-miR-185-5p, hsa-miR-584-5p, hsa-miR-32-5p, hsa-miR-142-3p, hsa-miR-425-3p, and hsa-miR-374a-3p — are currently not linked to known miRNA-targeting drugs extracted from DGIdb database. (For interpretation of the references to color in this figure legend, the reader is referred to the web version of this article.)

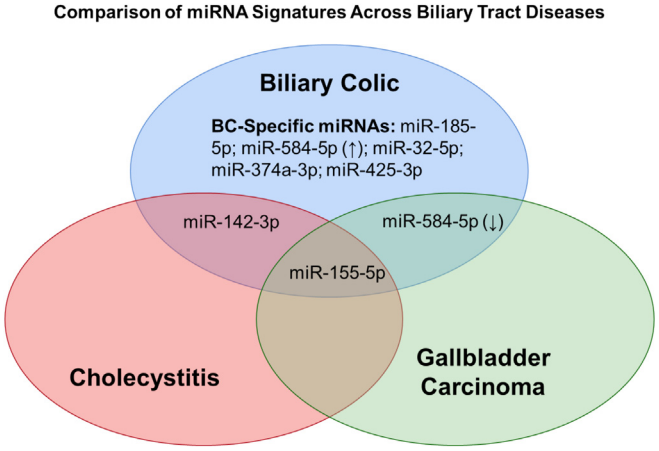

Fig. 8. Comparison of miRNA signatures across biliary tract diseases. Venn diagram showing overlap between miRNA signatures identified in our BC study compared with published signatures from cholecystitis, gallbladder carcinoma, and cholangiocarcinoma, highlighting BC-specific miRNAs and shared inflammatory mediators.

turquoise module, which showed a strong positive correlation with BC patients and a negative correlation with HC, emerged as a key module associated with BC pathogenesis. This suggests that the miRNAs within this module play critical roles in the molecular alterations observed in BC. Previous research has also emphasized the importance of co-expression networks in understanding complex diseases, as they provide insights into the interactions between genes and miRNAs that drive disease processes [29,30]. The strong association of the turquoise module with BC underlines the potential of miRNA modules in identifying disease-specific signatures and therapeutic targets.

Through the integration of differential expression analysis, WGCNA, and LASSO regression, we identified 7 key miRNAs (hsa-miR-142-3p, hsa-miR-32-5p, hsa-miR-374a-3p, hsa-miR-155-5p, hsa-miR-425-3p, hsa-miR-584-5p, and hsa-miR-185-5p) that are strongly associated with BC. These miRNAs are highly expressed in BC patients, and their expression patterns can serve as reliable biomarkers for disease diagnosis. Among these, hsa-miR-185-5p was found to have the highest odds ratio, suggesting its potential as a key diagnostic marker. Previous studies have reported the involvement of several of these miRNAs in other malignancies, such as hsa-miR-155-5p, which has been implicated in inflammatory and immune-related processes [31,32]. The strength of our

Table 4
Comparison of key miRNA expression in different biliary diseases.

miRNA	BC (Our Study)	Cholecystitis	Gallbladder Carcinoma	Cholangiocarcinoma	Reference
hsa-miR-155-5p	Upregulated	Upregulated	Upregulated	Upregulated	[16,27,28]
hsa-miR-185-5p	Upregulated	Not reported	Not reported	Not reported	–
hsa-miR-142-3p	Upregulated	Upregulated	Not reported	Upregulated	[27]
hsa-miR-32-5p	Upregulated	Not reported	Not reported	Not reported	–
hsa-miR-374a-3p	Upregulated	Not reported	Not reported	Not reported	–
hsa-miR-425-3p	Upregulated	Not reported	Not reported	Not reported	–
hsa-miR-584-5p	Upregulated	Not reported	Downregulated	Not reported	[16]

*This comparative analysis demonstrates that while some miRNAs like hsa-miR-155-5p are commonly dysregulated across biliary diseases, others like hsa-miR-185-5p and hsa-miR-584-5p appear more specific to BC, suggesting potential disease-specific biomarkers.

research's correlation between hsa-miR-155-5p and BC suggests that it may be used as a therapeutic target as well as a biomarker.

Our functional enrichment analysis revealed that targets of the identified key miRNAs are significantly involved in inflammatory response, pain signaling, and smooth muscle contraction pathways, all directly relevant to BC pathophysiology. For instance, hsa-miR-155-5p regulates NF-κB signaling, a central pathway in inflammation, while predicted targets of hsa-miR-185-5p are enriched in pain response pathways. Additionally, hsa-miR-32-5p targets genes involved in smooth muscle contraction, potentially contributing to the characteristic colicky pain of BC. These findings provide mechanistic insights into how these miRNAs may contribute to BC development and symptomatology, beyond their utility as biomarkers (Fig. 7, Table 2).

To further validate the diagnostic utility of these miRNAs, three machine learning techniques were used as models: LR, RF, and SVM. The SVM and RF models demonstrated perfect discrimination between BC and HC with an AUC of 1.0, while the LR model showed a slightly lower AUC of 0.875. These outcomes highlight how effective machine learning is in enhancing the predictive accuracy of biomarkers. The excellent performance of the SVM and RF models is particularly promising, as they offer potential for clinical applications, where accurate, early diagnosis of BC could lead to better patient outcomes. Previous studies have shown how well machine learning models anticipate a variety of diseases using miRNA signatures, reinforcing the value of combining advanced computational techniques with molecular biomarkers [33,34].

While our models showed excellent performance metrics, we acknowledge the potential for overfitting given our relatively small sample size. Our 5-fold cross-validation analysis resulted in slightly reduced but still strong performance metrics (cross-validated AUCs of 0.95 for SVM, 0.92 for RF, and 0.85 for LR), providing a more realistic assessment of model performance on unseen data. These findings suggest that while some degree of overfitting may be present, the identified miRNA signatures retain strong discriminatory power. Future studies with larger, independent cohorts will be crucial to fully validate these models (Fig. 5D, Table 3).

Beyond their diagnostic potential, the key miRNAs found in this investigation could also act as targets for therapy for BC. miRNA-based therapies are emerging as a promising strategy for treating various diseases, including cancer [35]. The miRNA-drug interaction network revealed that hsa-miR-155-5p is targeted by two therapeutic candidates, Remlarsen and Cobomarsen. These drugs have demonstrated potential in clinical trials for several illnesses, including cancer and autoimmune disorders, suggesting that targeting hsa-miR-155-5p could be an effective therapeutic approach for BC [36,37]. However, the other key miRNAs in our study (hsa-miR-185-5p, hsa-miR-584-5p, hsa-miR-32-5p, hsa-miR-142-3p, hsa-miR-425-3p, and hsa-miR-374a-3p) do not yet have any known targeted drugs, indicating a need for further research into potential therapeutic interventions.

One of the study's main weaknesses is its rather small sample size, which could limit how far the results can be applied. Furthermore, the lack of broader clinical validation poses a challenge in confirming the applicability of identified biomarkers in diverse patient populations. Potential batch effects during sample processing could also introduce variability in miRNA expression profiles. Despite our efforts to correct for batch effects using the Empirical Bayes method, some technical variability may persist. Additionally, the limited demographic information available in the public datasets prevented us from controlling for potential confounding factors such as age, sex, and comorbidities, which could influence miRNA expression patterns. The perfect discrimination achieved by our SVM and RF models may reflect some degree of overfitting, as suggested by our cross-validation analysis [38,39]. These limitations suggest a need for larger-scale studies that encompass varying demographics and clinical settings to robustly validate our findings as recommended in previous biomarker discovery studies [40,41].

In conclusion, this study highlights the possibilities for diagnosis and treatment of circulating exosomal miRNA signatures in BC. By identifying key miRNAs associated with BC and demonstrating their predictive power using machine learning models, we provide a solid foundation in order to create miRNA-based biomarkers for BC. Furthermore, the identification of therapeutic candidates targeting hsa-miR-155-5p offers new avenues for the treatment of BC. These findings underscore the need for further investigation into the clinical utility of exosomal miRNAs in BC and other biliary tract diseases. Future studies should concentrate on investigating these miRNAs' functional roles and validating them in larger cohorts the pathogenesis of BC to refine their potential for both diagnosis and therapy using advanced analytical techniques [42,43].

CRediT authorship contribution statement

Xiangjie Han: Writing – original draft. **Anshi Wu:** Resources. **Mengmeng Bao:** Supervision, Writing – review & editing, Project administration.

Informed consent

All patients obtained written informed consent.

Ethical approval

This study protocol was approved by the Ethics Committee of Beijing Chaoyang Hospital (CMUSTYH).

Financial support

This research was supported by the "Preliminary Exploration of Competency - Oriented DOPS - Combined with Hierarchical Teaching in the Standardized Anesthesia Training for Non - Anesthesia Resident Physicians Fund" (Project No. 2023028, General Program). The fund played a crucial role in enabling the study to be carried out smoothly, covering aspects such as data collection, research equipment procurement, and personnel costs.

Declaration of competing interest

The authors declare that they have no known competing financial interests or personal relationships that could have appeared to influence the work reported in this paper.

Acknowledgements

Thanks to all those who helped with the study but were not listed as co-authors due to insufficient contributions.

Supplementary material

https://doi.org/10.1016/j.ejbt.2025.05.007.

Data availability

Data will be made available on request.

References

[1] Demehri FR, Alam HB. Evidence-based management of common gallstone-related emergencies. J Intensive Care Med 2014;31(1):3–13. https://doi.org/10.1177/0885066614554192. PMid: 25320159.

[2] Chen SY, Huang HY, Lin HP, et al. Piperlongumine induces autophagy in biliary cancer cells via reactive oxygen species-activated Erk signaling pathway. Int J Mol Med 2019;44(5):1687–96. https://doi.org/10.3892/ijmm.2019.4324.

[3] Hucl T. Precursors to cholangiocarcinoma. Gastroenterol Res Pract 2019;2019 (1):1389289. https://doi.org/10.1155/2019/1389289. PMid: 31814823.

[4] Guévremont D, Roy J, Cutfield NJ, et al. MicroRNAs in Parkinson's disease: A systematic review and diagnostic accuracy meta-analysis. Sci Rep 2023;13:16272. https://doi.org/10.1038/s41598-023-43096-9.

[5] Huang S, Wang YJ, Guo J. Biofluid biomarkers of Alzheimer's disease: Progress, problems, and perspectives. Neurosci Bull 2022;38(6):677–91. https://doi.org/10.1007/s12264-022-00836-7. PMid: 35306613.

[6] Weidauer S, Wagner M, Hattingen E. White matter lesions in adults - A differential diagnostic approach. Rofo 2020;192(12):1154–73. https://doi.org/10.1055/a-1207-1006. PMid: 32688424.

[7] Peterson MF, Otoc N, Sethi JK, et al. Integrated systems for exosome investigation. Methods 2015;87:31–45. https://doi.org/10.1016/j.ymeth.2015.04.015. PMid: 25916618.

[8] McBride JD, Rodriguez-Menocal L, Badiavas EV. Extracellular vesicles as biomarkers and therapeutics in dermatology: A focus on exosomes. J Invest Dermatol 2017;137(8):1622–9. https://doi.org/10.1016/j.jid.2017.04.021. PMid: 28648952.

[9] Song X, Song Y, Zhang J, et al. Regulatory role of exosome-derived miRNAs and other contents in adipogenesis. Exp Cell Res 2024;441(1):114168. https://doi.org/10.1016/j.yexcr.2024.114168. PMid: 39004201.

[10] Kumar RMR. Exosomal microRNAs: Impact on cancer detection, treatment, and monitoring. Clin Transl Oncol 2025;27(1):83–94. https://doi.org/10.1007/s12094-024-03590-6. PMid: 38971914.

[11] Ankasha SJ, Shafiee MN, Wahab NA, et al. Post-transcriptional regulation of microRNAs in cancer: From prediction to validation. Oncol Rev 2018;12 (1):344. https://doi.org/10.4081/oncol.2018.344. PMid: 29989022.

[12] Tan PPS, Hall D, Chilian WM, et al. Exosomal microRNAs in the development of essential hypertension and its potential as biomarkers. Am J Phys Heart Circ Phys 2021;320(4):H1486–97. https://doi.org/10.1152/ajpheart.00888.2020. PMid: 33577433.

[13] Mishra PJ. MicroRNAs as promising biomarkers in cancer diagnostics. Biomark Res 2014;2:19. https://doi.org/10.1186/2050-7771-2-19. PMid: 25356314.

[14] Zafari S, Backes C, Leidinger P, et al. Regulatory microRNA networks: Complex patterns of target pathways for disease-related and housekeeping microRNAs. Genom Proteom Bioinform 2015;13(3):159–68. https://doi.org/10.1016/j.gpb.2015.02.004. PMid: 26169798.

[15] Lin H, Shi X, Li H, et al. Urinary exosomal miRNAs as biomarkers of bladder cancer and experimental verification of mechanism of miR-93-5p in bladder cancer. BMC Cancer 2021;21(1):1293. https://doi.org/10.1186/s12885-021-08926-x. PMid: 34861847.

[16] Yang P, Song F, Yang X, et al. Exosomal MicroRNA signature acts as an efficient biomarker for non-invasive diagnosis of gallbladder carcinoma. Science 2022;25(9). https://doi.org/10.1016/j.isci.2022.104816. PMid: 36043050.

[17] Arbelaiz A, Azkargorta M, Krawczyk M, et al. Serum extracellular vesicles contain protein biomarkers for primary sclerosing cholangitis and cholangiocarcinoma. Hepatology 2017;66(4):1125–43. https://doi.org/10.1002/hep.29291. PMid: 28555885.

[18] Høgdall D, O'Rourke CJ, Larsen FO, et al. Whole blood microRNAs capture systemic reprogramming and have diagnostic potential in patients with biliary tract cancer. J Hepatol 2022;77(4):1047–58. https://doi.org/10.1016/j.jhep.2022.05.036. PMid: 35750139.

[19] Taminau J, Meganck S, Lazar C, et al. Unlocking the potential of publicly available microarray data using inSilicoDb and inSilicoMerging R/Bioconductor packages. BMC Bioinf 2012;13:335. https://doi.org/10.1186/1471-2105-13-335. PMid: 23259851.

[20] Johnson WE, Li C, Rabinovic A. Adjusting batch effects in microarray expression data using empirical Bayes methods. Biostatistics 2007;8 (1):118–27. https://doi.org/10.1093/biostatistics/kxj037. PMid: 16632515.

[21] Ritchie ME, Phipson B, Wu D, et al. *limma* powers differential expression analyses for RNA-sequencing and microarray studies. Nucleic Acids Res 2015;43(7):e47. https://doi.org/10.1093/nar/gkv007. PMid: 25605792.

[22] Langfelder P, Horvath S. WGCNA: An R package for weighted correlation network analysis. BMC Bioinf 2008;9:559. https://doi.org/10.1186/1471-2105-9-559. PMid: 19114008.

[23] Gu Z, Eils R, Schlesner M. Complex heatmaps reveal patterns and correlations in multidimensional genomic data. Bioinformatics 2016;32(18):2847–9. https://doi.org/10.1093/bioinformatics/btw313. PMid: 27207943.

[24] Cannon M, Stevenson J, Stahl K, et al. DGIdb 5.0: Rebuilding the drug-gene interaction database for precision medicine and drug discovery platforms. Nucleic Acids Res 2024;52(D1):D1227–35. https://doi.org/10.1093/nar/gkad1040. PMid: 37953380.

[25] Kalluri R, LeBleu VS. The biology, function, and biomedical applications of exosomes. Science 2020;367(6478):eaau6977. https://doi.org/10.1126/science.aau6977. PMid: 32029601.

[26] Li B, Cao Y, Sun M, et al. Expression, regulation, and function of exosome-derived miRNAs in cancer progression and therapy. FASEB J 2021;35(10): e21916. https://doi.org/10.1096/fj.202100294RR.

[27] Letelier P, Riquelme I, Hernández AH, et al. Circulating MicroRNAs as biomarkers in biliary tract cancers. Int J Mol Sci 2016;17(5):791. https://doi.org/10.3390/ijms17050791. PMid: 27223281.

[28] Supradit K, Wongprasert K, Tangphatsornruang S, et al. microRNA profiling of exosomes derived from plasma and their potential as biomarkers for *Opisthorchis viverrini*-associated cholangiocarcinoma. Acta Trop 2024;258:107362. https://doi.org/10.1016/j.actatropica.2024.107362. PMid: 39151716.

[29] Qin D, Wei R, Liu S, et al. A circulating miRNA-based scoring system established by WGCNA to predict colon cancer. Anal Cell Pathol 2019;2019(1):1571045. https://doi.org/10.1155/2019/1571045. PMid: 31871878.

[30] Guo L, Cai Y, Wang B, et al. Characterization of the circulating transcriptome expression profile and identification of novel miRNA biomarkers in hypertrophic cardiomyopathy. Eur J Med Res 2023;28(1):205. https://doi.org/10.1186/s40001-023-01159-7. PMid: 37391825.

[31] Zanoaga O, Braicu C, Chiroi P, et al. The role of miR-155 in nutrition: Modulating cancer-associated inflammation. Nutrients 2021;13(7):2245. https://doi.org/10.3390/nu13072245. PMid: 34210046.

[32] Mohan S, Hakami MA, Dailah HG, et al. From inflammation to metastasis: The central role of miR-155 in modulating NF-κB in cancer. Pathol Res Pract 2024;253:154962. https://doi.org/10.1016/j.prp.2023.154962. PMid: 38006837.

[33] Abedi S, Behmanesh A, Mazhar FN, et al. Machine learning and experimental analyses identified miRNA expression models associated with metastatic osteosarcoma. Biochim Biophys Acta Mol basis Dis 2024;1870(7):167357. https://doi.org/10.1016/j.bbadis.2024.167357. PMid: 39033966.

[34] Aravind VA, Kouznetsova VL, Kesari S, et al. Using machine learning and miRNA for the diagnosis of esophageal cancer. J Appl Lab Med 2024;9 (4):684–95. https://doi.org/10.1093/jalm/jfae037. PMid: 38721901.

[35] He B, Zhao Z, Cai Q, et al. miRNA-based biomarkers, therapies, and resistance in cancer. Int J Biol Sci 2020;16(14):2628–47. https://doi.org/10.7150/ijbs.47203. PMid: 32792861.

[36] Gallant-Behm CL, Piper J, Lynch JM, et al. A microRNA-29 mimic (Remlarsen) represses extracellular matrix expression and fibroplasia in the skin. J Invest Dermatol 2019;139(5):1073–81. https://doi.org/10.1016/j.jid.2018.11.007. PMid: 30472058.

[37] Anastasiadou E, Seto AG, Beatty X, et al. Cobomarsen, an oligonucleotide inhibitor of miR-155, slows DLBCL tumor cell growth *in vitro* and *in vivo*. Clin Cancer Res 2021;27(4):1139–49. https://doi.org/10.1158/1078-0432.CCR-20-3139. PMid: 33208342.

[38] Chicco D, Jurman G. The advantages of the Matthews correlation coefficient (MCC) over F1 score and accuracy in binary classification evaluation. BMC Genomics 2020;21(1):6. https://doi.org/10.1186/s12864-019-6413-7. PMid: 31898477.

[39] Hastie T, Tibshirani R, Friedman J. The elements of statistical learning: Data mining, inference, and prediction. 2nd ed. New York: Springer; 2009.

[40] Freitas AA. Investigating the role of Simpson's paradox in the analysis of top-ranked features in high-dimensional bioinformatics datasets. Brief Bioinform 2020;21(2):421–8. https://doi.org/10.1093/bib/bby126. PMid: 30629111.

[41] Ding Y, Tang J, Guo F. Identification of drug–target interactions via dual Laplacian regularized least squares with multiple kernel fusion. Knowl Based Syst 2020;204:106254. https://doi.org/10.1016/j.knosys.2020.106254.

[42] Rupaimoole R, Slack FJ. MicroRNA therapeutics: Towards a new era for the management of cancer and other diseases. Nat Rev Drug Discov 2017;16 (3):203–22. https://doi.org/10.1038/nrd.2016.246. PMid: 28209991.

[43] Wei L, Ding Y, Su R, et al. Prediction of human protein subcellular localization using deep learning. J Parallel Distrib Comput 2018;117:212–7. https://doi.org/10.1016/j.jpdc.2017.08.009.